



Universiteit  
Leiden  
The Netherlands

## **Intestinal BMP-9 locally upregulates FGF19 and is down-regulated in obese patients with diabetes**

Drexler, S.; Cai, C.; Hartmann, A.L.; Moch, D.; Gaitantzi, H.; Ney, T.; ... ; Breitkopf-Heinlein, K.

### **Citation**

Drexler, S., Cai, C., Hartmann, A. L., Moch, D., Gaitantzi, H., Ney, T., ... Breitkopf-Heinlein, K. (2023). Intestinal BMP-9 locally upregulates FGF19 and is down-regulated in obese patients with diabetes. *Molecular And Cellular Endocrinology*, 570.  
doi:10.1016/j.mce.2023.111934

Version: Publisher's Version

License: [Creative Commons CC BY-NC-ND 4.0 license](https://creativecommons.org/licenses/by-nc-nd/4.0/)

Downloaded from: <https://hdl.handle.net/1887/3633702>

**Note:** To cite this publication please use the final published version (if applicable).



# Intestinal BMP-9 locally upregulates FGF19 and is down-regulated in obese patients with diabetes

Stephan Drexler<sup>a</sup>, Chen Cai<sup>a</sup>, Anna-Lena Hartmann<sup>b</sup>, Denise Moch<sup>b</sup>, Haristi Gaitantzi<sup>b</sup>, Theresa Ney<sup>b</sup>, Malin Kraemer<sup>b</sup>, Yuan Chu<sup>b</sup>, Yuwei Zheng<sup>b</sup>, Mohammad Rahbari<sup>c</sup>, Annalena Treffs<sup>b</sup>, Alena Reiser<sup>b</sup>, Bénédicte Lenoir<sup>d</sup>, Nektarios A. Valous<sup>d</sup>, Dirk Jäger<sup>d,e</sup>, Emrullah Birgin<sup>b</sup>, Tejas A. Sawant<sup>a</sup>, Qi Li<sup>f</sup>, Keshu Xu<sup>g</sup>, Lingyue Dong<sup>h</sup>, Mirko Otto<sup>b</sup>, Timo Itzel<sup>i,j</sup>, Andreas Teufel<sup>i,j</sup>, Norbert Gretz<sup>k</sup>, Lukas J.A.C. Hawinkels<sup>l</sup>, Aránzazu Sánchez<sup>m</sup>, Blanca Herrera<sup>m</sup>, Rudolf Schubert<sup>n</sup>, Han Moshage<sup>o</sup>, Christoph Reissfelder<sup>b,j</sup>, Matthias P.A. Ebert<sup>a,j</sup>, Nuh N. Rahbari<sup>b</sup>, Katja Bretkopf-Heinlein<sup>b,\*</sup>

<sup>a</sup> Department of Medicine II, University Medical Center Mannheim, Medical Faculty Mannheim, Heidelberg University, 68167, Mannheim, Germany

<sup>b</sup> Department of Surgery, University Medical Center Mannheim, Medical Faculty Mannheim, Heidelberg University, 68167, Mannheim, Germany

<sup>c</sup> German Cancer Research Center (DKFZ), Division of Chronic Inflammation and Cancer, 69120, Heidelberg, Germany

<sup>d</sup> Clinical Cooperation Unit „Applied Tumor Immunity“, German Cancer Research Center (DKFZ), 69120, Heidelberg, Germany

<sup>e</sup> Department of Medical Oncology, National Center for Tumor Diseases and Heidelberg University Hospital, 69120, Heidelberg, Germany

<sup>f</sup> Department of Gastroenterology and Hepatology, Beijing You'an Hospital Affiliated with Capital Medical University, Fengtai District, Beijing, China

<sup>g</sup> Division of Gastroenterology, Union Hospital, Tongji Medical College, Huazhong University of Science and Technology, 1277 Jiefang Av., Wuhan, Hubei, China

<sup>h</sup> Department of Cell Biology, Capital Medical University, Beijing, Fengtai, 100054, China

<sup>i</sup> Division of Hepatology, Division of Clinical Bioinformatics, Department of Medicine II, Medical Faculty Mannheim, Heidelberg University, 68167, Mannheim, Germany

<sup>j</sup> Clinical Cooperation Unit „Healthy Metabolism“, Center of Preventive Medicine and Digital Health, Medical Faculty Mannheim, 68167, Heidelberg University, Mannheim, Germany

<sup>k</sup> Medical Faculty Mannheim, Medical Research Center, Heidelberg University, 68167, Mannheim, Germany

<sup>l</sup> Department of Gastroenterology and Hepatology, Leiden University Medical Center, Albinusdreef 2, 2333 ZA, Leiden, the Netherlands

<sup>m</sup> Department of Biochemistry and Molecular Biology, Faculty of Pharmacy, Complutense University of Madrid (UCM), Health Research Institute Hospital Clínico San Carlos (IdISSC), E-28040, Madrid, Spain

<sup>n</sup> Physiology, Institute of Theoretical Medicine, Faculty of Medicine, University of Augsburg, 86159, Augsburg, Germany

<sup>o</sup> Department of Gastroenterology and Hepatology, University Medical Center Groningen, University of Groningen, 9712 CP, Groningen, the Netherlands

## ARTICLE INFO

### Keywords:

Diabetes  
BMP-9  
GDF2  
Obesity  
Liver steatosis  
LPS

## ABSTRACT

Bone morphogenetic protein (BMP)-9, a member of the TGF $\beta$ -family of cytokines, is believed to be mainly produced in the liver. The serum levels of BMP-9 were reported to be reduced in newly diagnosed diabetic patients and BMP-9 overexpression ameliorated steatosis in the high fat diet-induced obesity mouse model. Furthermore, injection of BMP-9 in mice enhanced expression of fibroblast growth factor (FGF)21. However, whether BMP-9 also regulates the expression of the related FGF19 is not clear. Because both FGF21 and 19 were described to protect the liver from steatosis, we have further investigated the role of BMP-9 in this context.

We first analyzed BMP-9 levels in the serum of streptozotocin (STZ)-induced diabetic rats (a model of type I diabetes) and confirmed that BMP-9 serum levels decrease during diabetes. Microarray analyses of RNA samples from hepatic and intestinal tissue from BMP-9 KO- and wild-type mice (C57/Bl6 background) pointed to basal expression of BMP-9 in both organs and revealed a down-regulation of hepatic Fgf21 and intestinal Fgf19 in the KO mice. Next, we analyzed BMP-9 levels in a cohort of obese patients with or without diabetes. Serum BMP-9 levels did not correlate with diabetes, but hepatic BMP-9 mRNA expression negatively correlated with steatosis in those patients that did not yet develop diabetes. Likewise, hepatic BMP-9 expression also negatively correlated with serum LPS levels. In situ hybridization analyses confirmed intestinal BMP-9 expression. Intestinal (but not hepatic) BMP-9 mRNA levels were decreased with diabetes and positively correlated with intestinal E-Cadherin expression. In vitro studies using organoids demonstrated that BMP-9 directly induces FGF19 in gut but not

\* Corresponding author.

E-mail address: [katja.bretkopf@medma.uni-heidelberg.de](mailto:katja.bretkopf@medma.uni-heidelberg.de) (K. Bretkopf-Heinlein).

<https://doi.org/10.1016/j.mce.2023.111934>

Received 5 December 2022; Received in revised form 6 April 2023; Accepted 16 April 2023

Available online 19 April 2023

0303-7207/© 2023 The Authors. Published by Elsevier B.V. This is an open access article under the CC BY-NC-ND license (<http://creativecommons.org/licenses/by-nc-nd/4.0/>).

hepatocyte organoids, whereas no evidence of a direct induction of hepatic FGF21 by BMP-9 was found. Consistent with the *in vitro* data, a correlation between intestinal BMP-9 and FGF19 mRNA expression was seen in the patients' samples.

In summary, our data confirm that BMP-9 is involved in diabetes development in humans and in the control of the FGF-axis. More importantly, our data imply that not only hepatic but also intestinal BMP-9 associates with diabetes and steatosis development and controls FGF19 expression. The data support the conclusion that increased levels of BMP-9 would most likely be beneficial under pre-steatotic conditions, making supplementation of BMP-9 an interesting new approach for future therapies aiming at prevention of the development of a metabolic syndrome and liver steatosis.

## 1. Introduction

The term "non-alcoholic fatty liver disease (NAFLD)" or, as it is newly termed "Metabolic dysfunction-associated fatty liver disease (MAFLD)" (Eslam et al., 2020), describes a range of hepatic disorders, characterized by an excessive hepatic accumulation of triglycerides. The etiology is multifactorial; however, important risk factors include the metabolic syndrome and diabetes (Angulo, 2002), (Moore, 2010). Parallel to the obesity epidemic, NAFLD prevalence is progressively increasing (Younossi et al., 2016). 20–30% of the world population suffers from NAFLD and approximately 60% of these patients already developed inflammatory non-alcoholic steatohepatitis (NASH) (Younossi et al., 2016). This and the current lack of effective therapies (Vizuite et al., 2017) has shifted the attention towards finding new NAFLD modifying agents.

Bone Morphogenetic Protein (BMP)-9 is a member of the Transforming Growth Factor (TGF)- $\beta$  family of cytokines. Currently more than 15 BMPs have been identified in mammals (Herrera et al., 2017). They are secreted glycoproteins, which are involved in many biological activities, including cell growth, cell differentiation and apoptosis. BMP-9 was intensely investigated in the context of organ fibrosis (Tang et al., 2020), including the liver (Breitkopf-Heinlein et al., 2017). Additionally, an increasing number of publications suggests a role for BMP-9 in glucose- and fat-metabolism (Chen et al., 2003; Kuo et al., 2014; Kim et al., 2016; Xu et al., 2017; Yang et al., 2019).

BMP-9 is produced by hepatic stellate cells in the liver (Breitkopf-Heinlein et al., 2017). It binds to heterotetrameric complexes composed of type 1 and type 2 serine/threonine kinase receptors localized in the cell membrane. There are five different type 1 receptors, termed activin-like kinase receptors (ALK1-5) and 3 BMP-type 2 receptors: ActRIIA, ActRIIB and BMPRII. BMP-9 binds with highest affinity to a complex of ALK1 and ActRIIB. Upon ligand binding, the two receptors phosphorylate each other, which leads to signal transduction involving phosphorylation of Smads -1, -5 and -8. Classical target genes of

BMP's, including BMP-9, are Id1 or hepcidin (Breitkopf-Heinlein et al., 2017; Townson et al., 2012; Truksa et al., 2006).

According to Xu et al. (2017) and Yang et al. (2019), BMP-9 serum levels are decreased in patients with metabolic syndrome or diabetes type 2, supporting the assumption that BMP-9 might be involved in the regulation of the homeostasis of glucose- and fat metabolism. Chen et al. (2003) reported that injection of BMP-9 in diabetic mice leads to a normalization of glucose serum levels and an induction of lipid metabolism. Kim et al. (2016) also found a beneficial effect of injecting a BMP-9 mimetic into high fat diet (HFD)-induced obese mice. Similar results were recently reported by Sun et al. who stated that BMP-9 might alleviate NAFLD in HFD-fed mice (Sun et al., 2020). The underlying mechanism might involve BMP-9 mediated browning of adipose tissue (Kuo et al., 2014) and induction of Fibroblast growth factor (FGF) 21 expression in the liver (Kim et al., 2016).

FGF21 and its related cytokine FGF19 (in mice: FGF15) are well known anti-diabetic mediators (Ye et al., 2015; Harrison et al., 2018; Babaknejad et al., 2018). FGF21 is a member of the FGF19 subfamily, which comprises FGF19, FGF21 and FGF23. In contrast to other members of the FGF family, all members of the FGF19 subfamily act in an endocrine fashion. Both, FGF21 and FGF19 have crucial roles in glucose- and lipid metabolism (Babaknejad et al., 2018; Potthoff et al., 2009, 2011; Ryan et al., 2013) and they improve insulin resistance (Huang et al., 2007). BMP-9 and FGF21 have been described to be connected. Thus, injection of BMP-9 in mice fed a HFD led to enhanced hepatic expression of FGF21<sup>11</sup> and CRISPR-Cas mediated BMP-9 knock-out mice spontaneously developed obesity and steatosis (Yang et al., 2020). FGF19 and FGF21 both signal via the same co-receptor, KLB (Goetz et al., 2007; Ogawa et al., 2007). Since FGF19 is reported to be mostly produced in the gut by activation of farnesoid X receptor (FXR) (Inagaki et al., 2005; Degirolamo et al., 2016) we were interested to investigate if this FGF-axis might be regulated via a gut-liver crosstalk involving BMP-9.

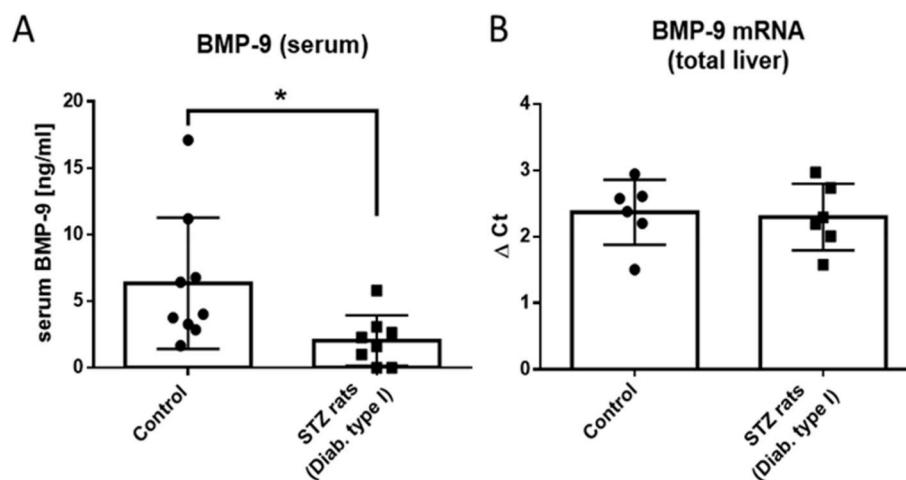


**Fig. 1. BMP-9 serum levels are decreased in STZ rats.** Rats were injected with streptozotocin (STZ) to cause a condition of diabetes type 1. A) The sera of the rats (n = 9 controls and 8 STZ-treated animals) were analyzed for BMP-9 protein levels by ELISA. B) Total RNA was isolated from the livers (n = 6 per group) and BMP-9 was determined by real-time PCR. Statistical differences were determined via Student's t-test.

We previously showed that presence of BMP-9 worsens hepatic fibrosis (Breitkopf-Heinlein et al., 2017) and enhances pro-inflammatory responses of macrophages (Gaitantzi et al., 2020). Whereas BMP-9 ameliorated HFD-induced steatosis (Yang et al., 2019), we recently demonstrated in the methionine and choline deficient (MCD) diet, a mouse-model resembling NASH, that overexpression of BMP-9 worsened liver damage, leading to enhanced serum levels of AST/ALT, increased fat deposition in the liver, as well as an enhanced invasion of pro-inflammatory, iNOS positive macrophages (Jiang et al., 2021).

Therefore, opposing effects of BMP-9 in steatotic, pre-diabetic, compared to already inflammatory and fibrotic conditions seem to exist. We hypothesized that BMP-9 may play different roles during the development of fatty liver/NAFLD compared to more severe stages of damage including inflammation/NASH. The molecular mechanisms of this complex actions of BMP-9 are not well understood up to now. The aim of the present study was therefore to specifically investigate if and how BMP-9 might modulate FGF19/FGF21 expression and signaling during hepatic fat accumulation before development of fulminant inflammation.

Our data point to a potential gut-liver crosstalk, in which locally produced intestinal BMP-9 causes an increase of FGF19 expression.

## 2. Materials and methods

### 2.1. Diabetic rats

Adult, 2- to 4-months-old male Wistar rats (Janvier, France) were employed (n = 9 controls and 8 STZ-treated animals). Food and water were available ad libitum, and the animals were housed in a room with a controlled temperature and a 12-h light-dark cycle. Diabetes was induced by injection of a single dose of streptozotocin (STZ), 35 mg/kg, in citrate buffer in the tail artery of the animals under isoflurane narcosis at an age of 8 weeks. Control animals received the same volume of citrate buffer. Eight weeks after STZ treatment, rats were sacrificed. Reduced body weight and enhanced serum glucose levels of STZ-treated mice were documented (Suppl. Fig 1). The investigation conformed with the US Guide for the Care and Use of Laboratory Animals (Eighth edition, National Academy of Sciences, 2011) and was approved by a governmental committee on animal welfare (Regierungspräsidium Karlsruhe) (G-208/14).

### 2.2. Mouse models of methionine- and choline-deficient diet (MCD) feeding and of adenoviral BMP-9 overexpression

Mouse models of MCD feeding and adenoviral BMP-9 overexpression were established as previously described (Li et al., 2019) and were performed in accordance with Hubei Province Laboratory Animal Care Guidelines for the use of animals in research and approved by the Animal Care and Use Committee at Tongji Medical College, Huazhong University of Science and Technology. The animals received humane care and were maintained in specific pathogen-free conditions. This protocol was approved in accordance with the guideline of the Ethics Committee of the Capital Medical University, Beijing, China.

### 2.3. BMP-9 knock-out mice

BMP-9-deficient mice were generated as previously described (Ricard et al., 2012). All experimental animal protocols were performed in accordance with directive 2010/63/EU and approved by local committees.

### 2.4. Human adipose patients' samples

All samples were collected at University Hospital Mannheim. Tissue procurement was approved by the local Medical Ethics Committees

(Reference no. 2016-607N-MA) and informed consent was obtained from all patients.

### 2.5. In situ hybridization of BMP-9 in human liver- and small intestine tissues

Tissue samples of adipose patients who underwent bariatric surgery (see Table 1) were fixed in formalin and embedded in paraffin using standard procedures. 2–7 days before hybridization the paraffin blocks were cut into 3 µm sections using a microtome and mounted on Superfrost® plus slides. Then the slides were baked for 1 h at 60 °C in a dry oven and stored at room temperature. In situ hybridization was performed using the RNAscope® Multiplex Fluorescent Reagent kit v2 (Advanced Cell Diagnostics, Inc., BioTechne, Minneapolis, MN, USA) according to the user manual. For signal development Opal™570 dye was used at a dilution of 1:1500. The tissue sections were examined under a Nikon Eclipse Ni-E microscope at 20–50X magnification. Stained slides were scanned using an Olympus VS200 slide scanner.

### 2.6. Upcyte® hepatocytes

Cryopreserved upcyte® human hepatocytes (upcHC) were obtained from Upcyte Technologies (Hamburg) and cultured according to the manufacturer's recommendations using their proprietary reagents, on 162 cm<sup>2</sup> sized, tissue culture flasks (CELLSTAR®, Greiner bio-one). 24 h before treatment, the cells were seeded on 3.5 cm plates at a density of  $2 \times 10^5$  cells/plate. For experiments with upcHC High Performance Medium® was used. All cultures were incubated at 37 °C and 5% CO<sub>2</sub>.

### 2.7. Generation of upcyte® hepatocyte organoids

$2 \times 10^5$  upcHC (cultured as described above) were mixed with 100 µL Matrigel® and plated in small drops on a suspension plate. After placing the plate upside down in the incubator for 45 min, the cultures were incubated in Hepatocyte Growth Medium (Upcyte Technologies) at 37 °C, 5% CO<sub>2</sub>. Prior to the experiments, the organoids were washed twice with PBS (pH = 7.4) and the medium was changed to High Performance Medium (Upcyte Technologies).

### 2.8. Human gut organoid generation and culture

Organoid cultures of human epithelial colon cells were derived from biopsies, as reported by Cai et al. (2022). Every 7–10 days the organoids were passaged.

### 2.9. Analyses of serum parameters of mice

Serum samples of BMP-KO mice were taken at the age of 4–5 months and the serum levels for the indicated parameters were measured according to standard protocols.

### 2.10. Affymetrix microarray analyses

Gene expression profiling was performed using arrays of ClariomTM S Human Arrays (Thermo Fisher Scientific, Waltham, MA, USA) as described previously (Gaitantzi et al., 2020). After normalizing the data by Robust Multichip Average algorithm (RMA) (Carvalho and Irizarry, 2010), multiple probes representing the same symbol were averaged for each array separately. Differential expressions were calculated as described by the limma package (Ritchie et al., 2015).

### 2.11. BMP-9, FGF19 and LPS ELISAs

The BMP-9 ELISA using rat serum samples was performed as previously described (van Baardewijk et al., 2013; Paauwe et al., 2016). In short, plates were coated with BMP-9 capture antibodies and 50 µl

**Table 1**

**Details of the cohort of adipose patients.** Samples from a cohort of 27 adipose patients were preserved. The patients received bariatric surgery during which tissue samples from liver and small intestine (jejunum) were obtained. Blood samples were taken before the operation. The NAFLD Activity Score (NAS) is a histological score, which combines steatosis, hepatocytes ballooning and lobular inflammation. BMI: body mass index; AST: aspartate aminotransferase; ALT: alanine aminotransferase; TAG: triacyl glycerides; Average values  $\pm$  SD (in brackets) are given.

	non-diabetes (n = 11)	diabetes (n = 16)
Age (years)	46.5 (13)	50.4 (9.3)
Gender (f/m)	10/1	12/4
NAS	3.6 (1.4)	3.5 (1.8)
BMI (kg/m <sup>2</sup> )	45.9 (5.5)	43 (3)
AST (U/l)	30.6 (12)	40.3 (16.2)
ALT (U/l)	38.5 (11.8)	58.5 (27)
TAG (mg/dl)	168.5 (80.5)	269.9 (213.4)
Albumin (g/l)	38.7 (2.5)	39.4 (2.9)

plasma samples diluted with 1% BSA/PBS or standard were incubated for 2h. After incubation with detection antibodies, color development was measured at 450 nm.

For detection of LPS, BMP-9 or FGF19 in human serum, the venous blood was centrifuged and only the serum was stored at  $-80^{\circ}\text{C}$  until biochemical determination. Serum levels were quantified following the instructions of the commercially available ELISA Kits: Cusabio, Human Lipopolysaccharides, LPS ELISA KIT and SimpleStep® ELISA Kits from Abcam (ab230943 and ab272470). The absorbance of the samples was measured at 450 nm and all serum samples were analyzed in duplicates.

## 2.12. Stimulation with fatty acids (FA)

Oleic (OA) and linoleic acids (LA) were dissolved in ethanol, palmitic acid (PA) was dissolved in methanol. The control condition contained the same amount of alcohol that was necessary to dissolve the fatty acids. 100 mM stock solutions of each FA were mixed with medium to reach the requested final concentrations. Usually, final concentrations amounted to 200  $\mu\text{M}$ , except the combination of PA + OA, which reached a combined final concentration of 400  $\mu\text{M}$ . In some trials a mix of PA, OA and LA in equal parts to final combined concentration of 200  $\mu\text{M}$  was used.

## 2.13. BMP-9 stimulation in vitro

5 ng/ml of recombinant BMP-9 (Peprotech) was used.

## 2.14. Real-time PCR

As described by Gaitantzi et al. (2020), total RNA was isolated using the peqGOLD Total RNA purification kit (Pepqlab) according to the

manufacturer's guidance. Using the SensiFAST™ cDNA Synthesis Kit (Bioline), total RNA was reverse transcribed to cDNA. Real time quantitative PCR (RT-qPCR) was accomplished according to the Analytik Jena innuMIX qPCR Master mix SyGreen protocol (Jena, Germany). Primer sequences used for RT-PCR are given in Table 2. Ct-values for each gene were first normalized to the average of all samples per experiment and the resulting values were then normalized to those of an appropriate housekeeping gene).

## 2.15. Statistics

All data are expressed as mean values  $\pm$  SD, n reflects biological replicates. For comparisons between two groups two-sided, unpaired Student's t-tests or ANOVA (as indicated in the legends) were used to detect significant differences. Categorization of significances was determined as follows:  $p < 0.05 = *$ ;  $p < 0.01 = **$ ;  $p < 0.001 = ***$ ;  $p < 0.0001 = ****$ .

Pearson correlations were calculated to define relationships between two parameters. The relationship was graded using the Pearson correlation "r" (see Table 3).

## 3. Results

### 3.1. Effects of constitutive deletion of BMP-9 in mice

We initially investigated the effects of the complete lack of BMP-9 in mice. BMP-9 knock-out (KO) mice were generated as described previously (Ricard et al., 2012). In contrast to a previously published work describing the phenotype of BMP-9 KO mice generated by CRISPR-Cas technology (Yang et al., 2020), our mice do not show any obvious hepatic steatosis and many serum-parameters of disease were not profoundly altered (Suppl. Fig. 2). However, the levels of glucose, cholinesterase and alkaline phosphatase were enhanced and the liver/body weight ratio was reduced, pointing to a possible pre-diabetic condition also in our KO-mice.

**Table 3**

**Relationship of grading and Pearson correlation "r".** Significance of correlations was further evaluated by student's t-test (using a significance level  $\alpha = 0.05$ ).

r value	grading
0.9 to 1 (−0.9 to −1)	very high pos. (neg.) correlation
0.7 to 0.9 (−0.7 to −0.9)	high pos. (neg.) correlation
0.5 to 0.7 (−0.5 to −0.7)	moderate pos. (neg.) correlation
0.3 to 0.5 (−0.3 to −0.5)	low pos. (neg.) correlation
0 to 0.3 (0 to −0.3)	negligible pos. (neg.) correlation

**Table 2**

Sequences of the primers used for real-time PCR. BMP-9, bone morphogenetic protein 9; FGF21, fibroblast growth factor 21; FGF19, fibroblast growth factor 19; KLB:  $\beta$ -klotho; B2M,  $\beta$ 2-microglobulin; Rpl19, 60S ribosomal protein L19; RS18, Ribosomal Protein S18; h = human; m = mouse; r = rat.

Target gene	Forward sequence (5' => 3')	Reverse sequence (5' => 3')
hBMP9	CGTCCAACATTGTGCGGAG	GACAGGAGACATAGAGTCGGAG
hFGF21	ACCAGAGCCCCGAAAGTCT	CTTGACTCCCAAGATTGAATAACTC
hFGF19	GCACAGTTTGCTGGA	ATCTCCTCTCGAAA
hB2M	GACTTGTCTTTCAGCAAGGA	ACAAAGTCACATGGTTTCA
hRS18	CCATTGCAACGTCTGCCCTAT	TCACCCGTGGTCACCATG
hCDH1	TGAAGGTGACAGAGCCTCTGGAT	TGGGTGAATTCGGGCTTGTT
rBMP9	AAGGGACCAAGTTGCCATTG	CAGACCCATATACCCAGTCA
rGAPDH	GAGTCAACGGATTGTGTCGT	GACAAGCTTCCCGTTCTCAG
mFgf21	CTACCAAGCATACCCATCC	GCCTACCACTGTTCCATCCT
mFgf15	ATGGCGAGAAAGTGGAAACGG	CTGACACAGACTGGGATTGCT
mB2m	TTCTGGTGCTGTCTCACTGA	CAGTATGTTGGGCTTCCCATTC



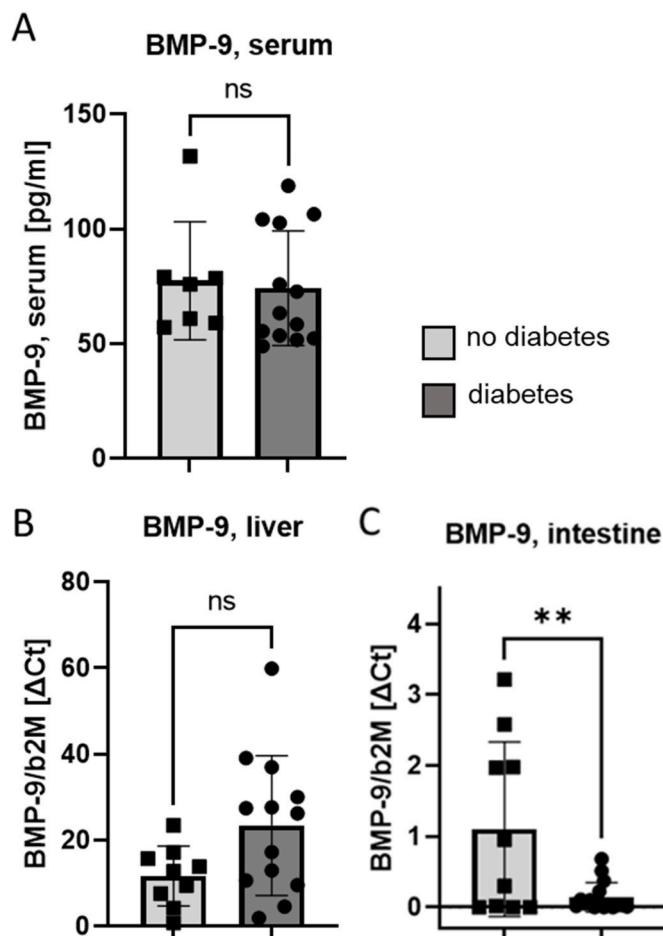


**Fig. 2.** BMP-9 levels in serum, liver and small intestine from adipose patients with or without diabetes. A) The sera of patients were analyzed for BMP-9 protein levels by ELISA measurement. Total RNA was isolated from samples of livers (B) and small intestine (C) and BMP-9 mRNA levels were determined by real-time PCR. Two -sided, unpaired Student's t-tests was used to detect significant differences.

### 3.2. Serum levels of BMP-9 are decreased in diabetic rats

BMP-9 was originally described as an autocrine/paracrine factor in the liver (Miller et al., 2000). More recent studies indicate a possible function of BMP-9 in the regulation of lipid and glucose metabolism (Xu et al., 2017; Yang et al., 2019). In this context, we measured protein levels of BMP-9 in the serum of diabetic rats. Diabetes was induced by treatment of the animals with streptozotocin (STZ) for 8 weeks which led to significantly increased blood glucose levels (Suppl. Figure 1). Compared to the healthy control group, BMP-9 levels were decreased in the diabetic animals (Fig. 1A).

To investigate if this decrease was accompanied by down-regulated hepatic expression, we next analyzed the mRNA levels of BMP-9 in the liver by real-time PCR. No differences were detected between control and diabetic conditions (Fig. 1B).

Thereby our data confirm previous reports of reduced BMP-9 in the serum of diabetic patients or mice (Xu et al., 2017). Nevertheless, in the STZ-rats this was not accompanied by reduced expression in the liver.

### 3.3. Correlation of BMP-9 levels with diabetes and steatosis in samples of adipose patients

In an attempt to obtain human data, we collected patient samples from a small cohort of adipose patients (with a BMI higher than 40) who

underwent bariatric surgery in our clinic (n = 27 in total). As depicted in Table 1, 16 of these adipose patients were already diagnosed with having diabetes. Age and NAS score was similar in both groups, whereas serum levels of liver function parameters (AST and ALT) as well as triglyceride levels (TAG) were higher in the diabetic group. From a total of 20 patients (7 non-diabetic and 13 diabetic) we performed ELISA analyses for the quantifications of serum BMP-9, FGF19 and lipopolysaccharide (LPS). Tissue samples from small intestine (jejunum; n = 26; 10 non-diabetic and 16 diabetic) and liver (n = 22; 9 non-diabetic and 13 diabetic) were processed for RNA isolation and subsequent real-time PCR analyses.

When measuring BMP-9 protein levels in the serum as well as hepatic and intestinal BMP-9 mRNA expressions in both groups we did neither find any significant difference in BMP-9 protein levels in the serum (Fig. 2A) nor in the hepatic mRNA levels (Fig. 2B). In contrast, we detected a significant decrease in intestinal BMP-9 mRNA levels in the diabetic patients' samples (Fig. 2C).

These data imply that hepatic BMP-9 expression might not necessarily correlate with an existing diabetic condition, at least when comparing groups of already adipose patients, but that there is an additional BMP-9 expression in the small intestine and this source of BMP-9 is indeed reduced in diabetic patients.

In order to get some more hints about the role of BMP-9 in vivo, we collected tissue samples from the liver, the colon, and the small intestine of wild type and BMP-9 KO mice and investigated changes in gene expression levels by Affymetrix microarray analyses. Since this was meant to be a preliminary screen of genome-wide changes, samples from 6 mice per group were pooled before analyses.

The results point to two interesting conclusions: 1. In accordance with the above described findings, there was a substantial basal BMP-9 expression level not only in the liver but also in the small intestine and, at lower levels, in the colon. 2. Absence of BMP-9 clearly affected the FGF-axis: hepatic Fgf21 as well as intestinal Fgf15 (the mammalian analogue of FGF19) were decreased in the KO mice (Suppl. Fig. 3).

In summary, these data from human as well as mouse samples imply that besides hepatic BMP-9 expression also intestinal levels exist and might be important during diabetes induction. Furthermore, although our BMP-9 KO mice are not obese, at the time of analysis, they already show a clearly disturbed balance of the FGF-axis in intestine and liver.

### 3.4. BMP-9 mRNA is detectable in human small intestine in non-epithelial cells

In consequence of these findings, we next aimed at confirming that there is indeed expression of BMP-9 mRNA in human small intestine. For this we performed in situ hybridization (using RNA Scope®) on human liver and intestine sections. The results confirm that basal expression of BMP-9 mRNA is clearly detectable in human jejunum (Fig. 3).

In the liver the morphology of BMP-9 expressing cells fits well with hepatic stellate cells as cellular source of BMP-9, as it has been described by us before (Breitkopf-Heinlein et al., 2017). Positive cells in the small intestine were rather small and round, were non-epithelial and did not directly localize to blood vessels (Fig. 3). Although the exact nature of these cells still needs to be defined, by morphology they might be myeloid-derived cells like dendritic cells or macrophages but rather not fibroblasts, endothelial or epithelial cells.

These results further support the concept of a relevant basal BMP-9 expression in the intestine.

### 3.5. BMP-9 induces FGF19 in gut epithelial cells in vitro

To analyse if BMP-9 – alone or in combination with fatty acids (FA) – directly regulates FGF19 expression in human hepatocytes, monolayer cultures were treated with recombinant BMP-9 and/or FA in vitro and were analyzed for FGF19 expression by rt-PCR. We could not detect any significant change of FGF19 expression upon stimulation with BMP-9,

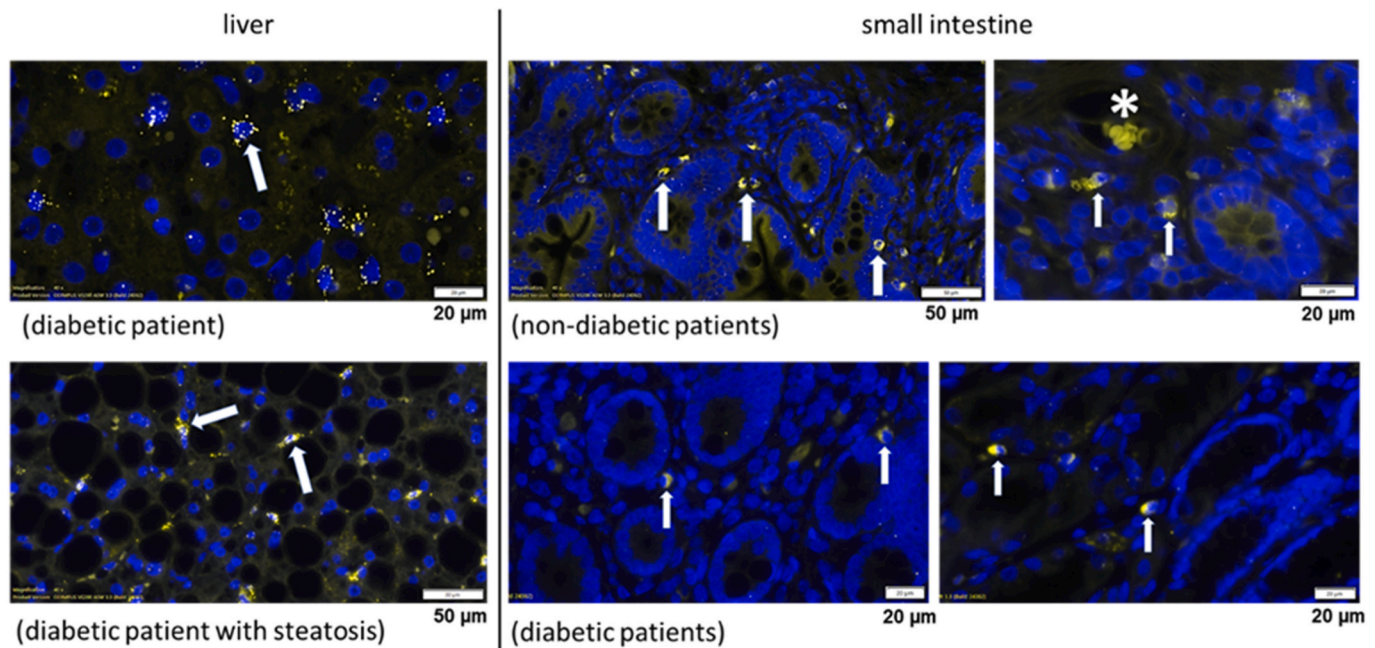


**Fig. 3.** In situ hybridization (RNA-Scope®) showing BMP-9 positive cells in human liver and gut. Tissue samples were collected from a cohort of adipose patients who underwent bariatric surgery in our clinic. In situ hybridization was performed using RNA Scope®. BMP-9 positive cells (yellow) are marked with white arrows. As \* marked structure shows false-positive platelets within blood vessels. The cell nuclei were counter-stained with DAPI.

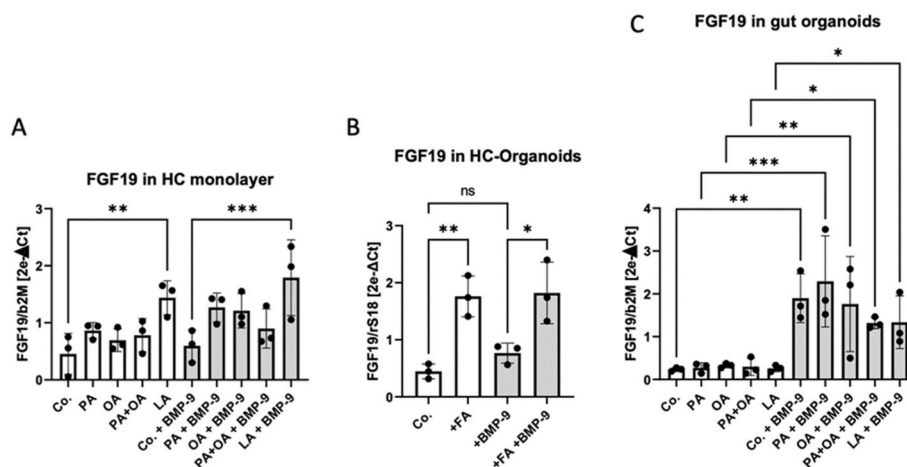


**Fig. 4.** Regulation of FGF19 expression by BMP-9 and fatty acids in hepatocytes and gut organoids. A) UpcHC were cultured as monolayer. After 4 h of serum starvation (0.5% FCS), stimulation for 48 h was performed with different fatty acids like PA, OA and LA (final concentration of 200 mM, except PA + OA, which reached a final cumulative concentration of 400 mM). For BMP-9 exposure, a concentration of 5 ng/ml was used. FGF19 expression was measured by rt-PCR. B) UpcHC were mixed with matrigel and after 48h, the formed organoids were stimulated with a mix of fatty acids (PA, OA and LA in equal parts, cumulative concentration: 200 mM), or BMP-9 (5 ng/ml) or both for another 48h. FGF19 expression was measured by rt-PCR. C) Epithelial cells were isolated from human resected (non-malignant) colon tissue and were mixed with matrigel. After formation, the organoids were stimulated like in A) for 48 h mRNA levels of FGF19 were again determined by rt-PCR. BMP-9, bone morphogenetic protein-9; Co, control; PA, palmitic acid; OA, oleic acid; LA, linoleic acid; FA, fatty acid mix; b2M,  $\beta$ 2-microglobulin; rS18, ribosomal protein 18; rpl19, 60S-protein L19; FGF19, fibroblast growth factor 19, FGF21, fibroblast growth factor 21.

whereas linoleic acid (LA) did (Fig. 4A). Since monolayer cultured hepatocytes are known to dedifferentiate fast (Rowe et al., 2013; Godoy et al., 2009), we sought to use a more physiological culture condition and generated organoids. Consistent with data in standard cultured hepatocytes, BMP-9 did not induce FGF19 expression in 3D culture conditions, but FA stimulation did (Fig. 4B). In gut organoid cultures, in contrast, BMP-9 clearly induced FGF19 expression (Fig. 4C). Fatty acids induced FGF19 only in hepatocytes but not in gut organoids.

In line with a BMP-9 mediated induction of FGF19 in the gut, we also found that intestinal (but not hepatic) BMP-9 mRNA levels positively correlated with intestinal FGF19 expression in our patient samples. FGF19 serum levels, however, did not correlate with BMP-9 expression (Fig. 5).

Interestingly, at least in our small cohort, the levels of circulating

BMP-9 protein did neither directly correlate with hepatic nor with intestinal BMP-9 expression. Neither did serum BMP-9 directly correlate with serum FGF19 (Suppl. Fig. 4). These data imply that local BMP-9 in the small intestine might be more relevant for FGF19 expression than circulating BMP-9. However, the possibility exists of course, that there are additional sources of BMP-9 that might also contribute to serum BMP-9 levels, this possibility remains to be investigated.

### 3.6. Intestinal BMP-9 expression is positively correlated with E-Cadherin

To further analyse the connection of intestinal BMP-9 expression with features of diabetes we measured the expression levels of E-Cadherin. Lack of E-Cadherin in mice was described to be related to a compromised intestinal barrier function (Bondow et al., 2012).

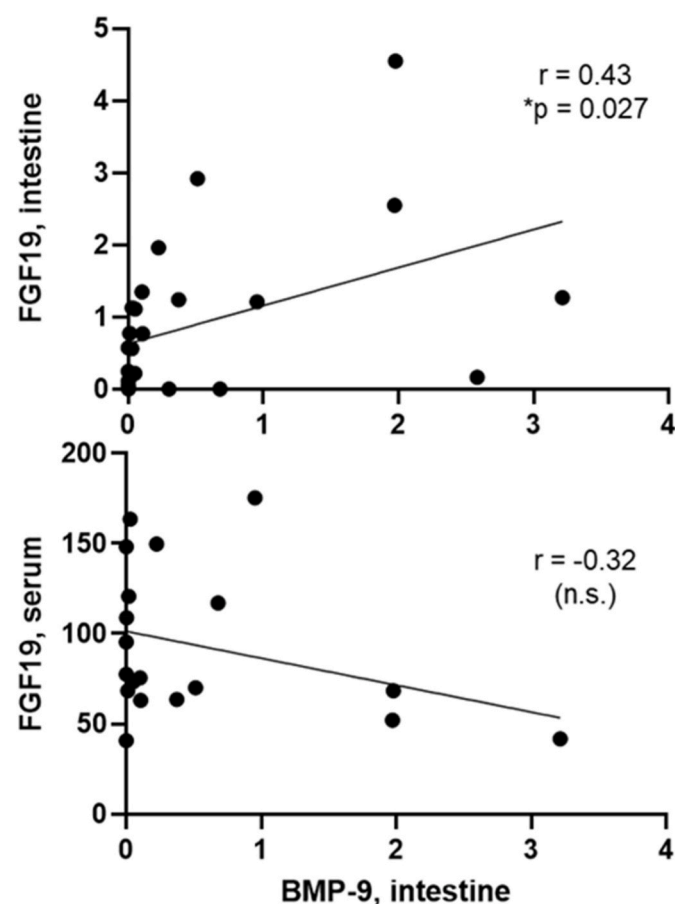


Fig. 5. Intestinal BMP-9 mRNA levels positively correlate with intestinal FGF19 expression but not with serum levels of FGF19 in adipose patients with or without diabetes. Total RNA was isolated from samples of small intestine and BMP-9 and FGF19 mRNA levels were determined by rt-PCR. FGF19 protein levels were determined in serum samples of the same patients (n = 19). n.s., not significant.

Accordingly, E-Cadherin expression was significantly lower in the intestine samples of the diabetic patients (Fig. 6A). Interestingly local BMP-9 expression directly correlated with that of E-Cadherin in the intestine (Fig. 6B). To test whether E-Cadherin might be directly targeted

by BMP-9 and/or fatty acids, PCR analyses were performed with the same gut organoid samples as before (see Fig. 4C). The results clearly show that there is no direct effect of BMP-9 or fatty acids on E-Cadherin expression in these intestinal epithelial cell cultures (Suppl. Fig. 5).

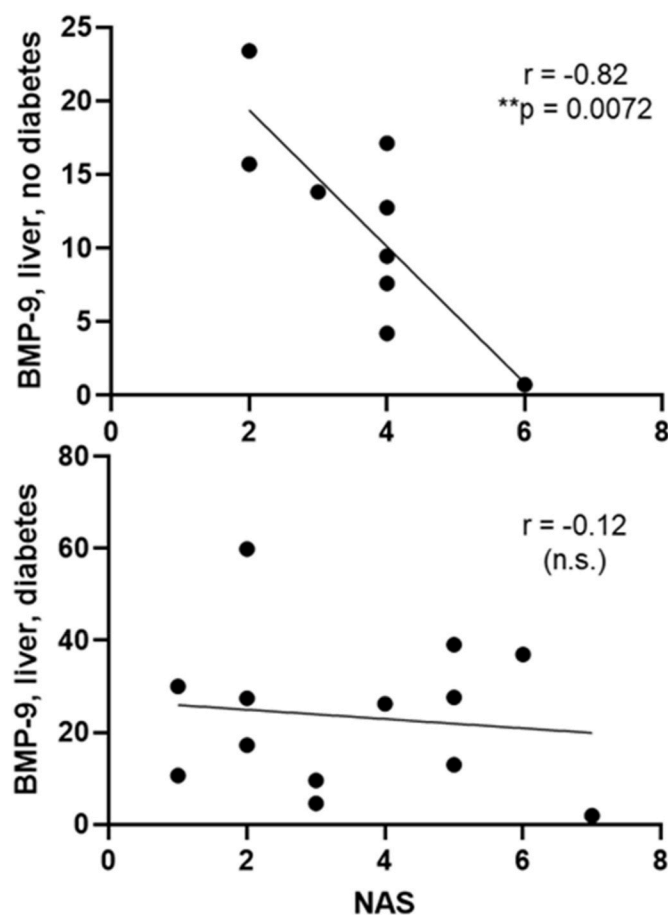


Fig. 7. Hepatic BMP-9 mRNA levels negatively correlate with NAS steatosis score in non-diabetic patients. Total RNA was isolated from liver samples of adipose patients with (n = 13) or without diabetes (n = 9) and BMP-9 mRNA levels were determined by rt-PCR. The resulting values were correlated with the NAS steatosis score for each patient individually. n.s., not significant.

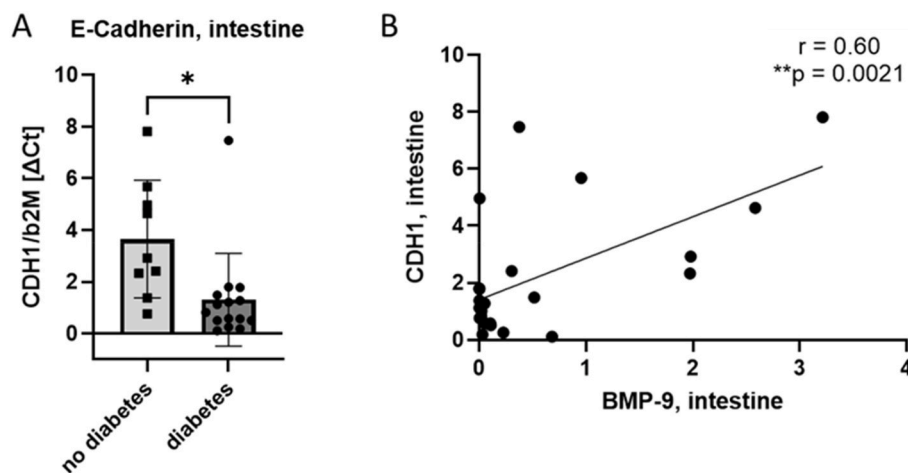
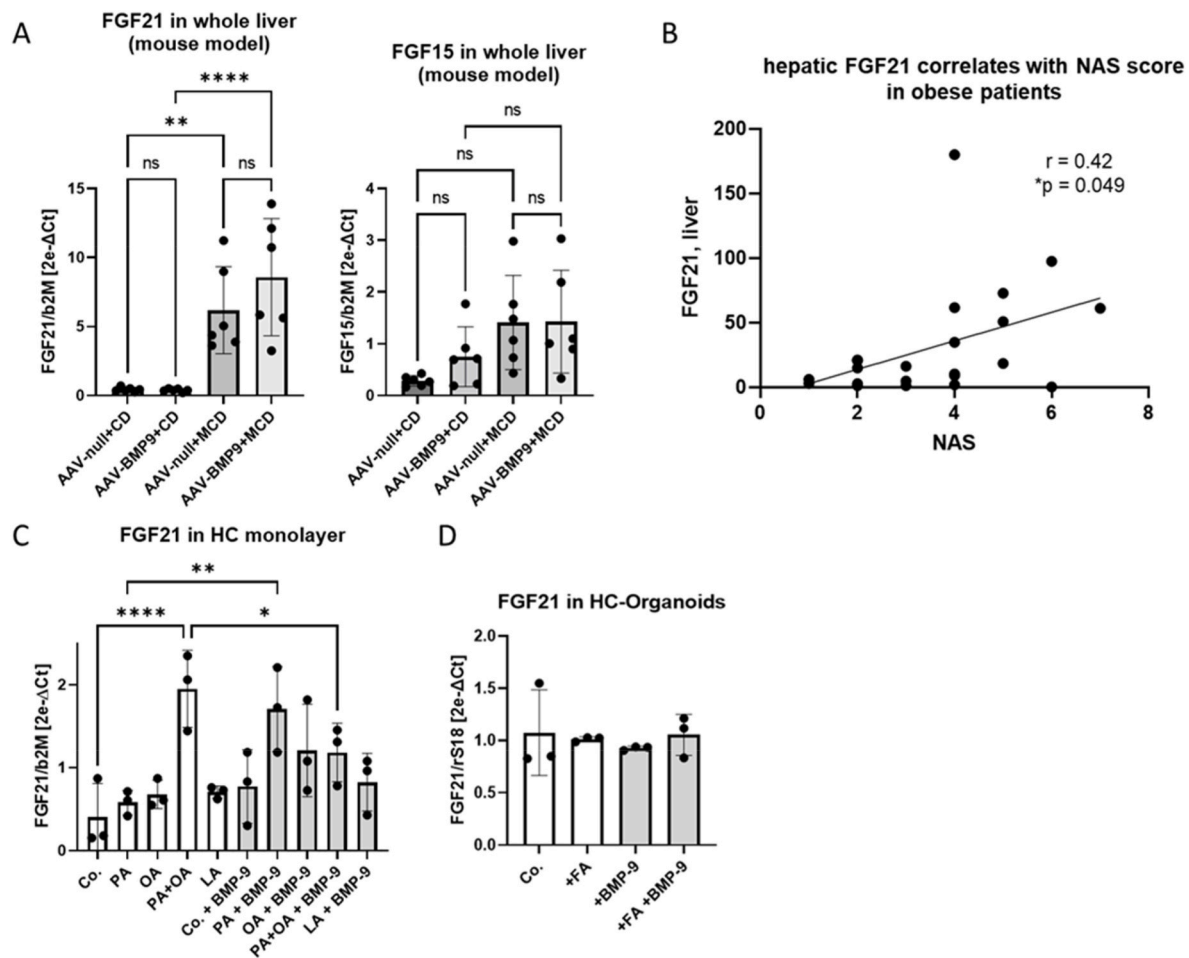


Fig. 6. Intestinal E-Cadherin mRNA levels are decreased in adipose patients with diabetes and are correlating with BMP-9 expression. Total RNA was isolated from samples of small intestine and E-Cadherin (CDH1) mRNA levels were determined by rt-PCR. A) E-Cadherin levels were significantly reduced in the samples from diabetic patients. B) Intestinal BMP-9 expression was positively correlating with that of E-Cadherin (all patients).





**Fig. 8. BMP-9 does not directly induce hepatic FGF-21 expression.** A) Healthy mice were infected with a BMP-9 overexpressing adeno-associated virus (AAV-BMP9; one injection per week for four weeks) as indicated. Additionally, one group of mice was exposed to a methionine and choline deficiency (MCD) diet for 24 weeks. Animals were sacrificed and the livers were obtained for analysis of mRNA expression levels of FGF21 and FGF15 via rt-PCR. B) Total RNA was obtained from livers of obese patients. FGF21 was measured by rt-PCR and was correlated to the NAS score. C) UpcHC, a non-malignant cell line derived from primary human hepatocytes, were cultured following the recommendations of Upcyte Technologies. After 4 h of serum starvation (0.5% FCS), stimulation for 48 h was performed with different fatty acids like PA, OA and LA (final concentration 200  $\mu$ M, except PA + OA, which reached a final cumulative concentration of 400  $\mu$ M). For BMP-9 exposure, a concentration of 5 ng/ml was used and FGF21 expression was analyzed by rt-PCR. D) UpcHC were cultured in 3D as organoids in matrigel. After 48 h, the organoids were stimulated with a mix of fatty acids (PA, OA and LA in equal parts, cumulative concentration of 200  $\mu$ M), or BMP-9 (5 ng/ml) or both and FGF21 expression was again analyzed by rt-PCR. BMP-9, bone morphogenetic protein-9, Co, control; CD, control diet; MCD, methionine and choline deficient diet; PA, palmitic acid; OA, oleic acid; LA, linoleic acid; FA, fatty acid mix; b2M,  $\beta$ 2-microglobulin; rS18, ribosomal protein 18; FGF15, fibroblast growth factor 15, FGF21, fibroblast growth factor 21. Data are expressed as average values  $\pm$  SD. Statistics were calculated by Student's t-test (A) or Pearson correlation (B) or ANOVA (C and D).

Nevertheless, the correlation between intestinal BMP-9 and E-Cadherin expression further supports the hypothesis that local BMP-9 levels in the intestine may be involved in the pathogenesis of metabolic syndrome/diabetes.

### 3.7. Hepatic BMP-9 mRNA levels negatively correlate with NAS steatosis score in non-diabetic patients

Following our hypothesis that BMP-9 might be a protective factor, we next analyzed if hepatic BMP-9 expression correlates with liver steatosis. For this purpose, we performed correlation analyses for hepatic BMP-9 mRNA levels compared to the individual degree of steatosis, measured by the NAS score. As shown in [Fig. 7](#), we found that hepatic BMP-9 levels were indeed highly negatively correlated with NAS, but only in the subgroup of non-diabetic patients. If diabetes had already developed, hepatic BMP-9 did not correlate with NAS any more. This could imply that high hepatic BMP-9 could have protective effects that get lost after diabetes has already developed.

We previously found that BMP-9 itself is directly down-regulated by LPS in hepatic stellate cells (HSC) (Breitkopf-Heinlein et al., 2017) and since LPS levels can be expected to be increased in steatotic and/or diabetic patients (Jayashree et al., 2014; Carpino et al., 2020), we also measured LPS levels in the serum samples of our patient cohort. As expected, we found a negative correlation between hepatic BMP-9 and serum LPS levels, which was more pronounced in diabetic patients (Suppl. Fig. 6). However, this negative correlation did not reach statistical significance in our patient cohort.

### 3.8. Hepatic FGF21 expression positively correlates with liver steatosis but is not directly regulated by BMP-9

Since injection of the BMP-9 mimetic MB109 enhanced hepatic expression of FGF21 *in vivo* in obese mice (Kim et al., 2016) and because we saw reduced FGF21 expression in the livers of our BMP-9 KO mice (Suppl. Fig. 3), it was assumed that BMP-9 directly induces FGF21 mRNA expression in liver cells. To test this hypothesis, we first analyzed

the hepatic expression levels of FGF21 in vivo in a mouse model of steatosis. In contrast to the published data using the BMP-9 mimetic in obese mice, infecting healthy, non-obese mice with a BMP-9 over-expressing adeno-associated virus (AAV-BMP9; one injection per week for four weeks) did not cause enhanced hepatic expression of FGF21 (Fig. 8A). Only the condition of methionine and choline deficiency (MCD) diet significantly enhanced FGF21 expression. The latter had been reported before (Tanaka et al., 2015). Additional overexpression of BMP-9 in MCD diet fed mice did not promote this upregulation any further (Fig. 8A). In line with the data from MCD diet, in the patient samples the NAS score was positively correlated with hepatic FGF21 expression (Fig. 8B). Levels of hepatic FGF15 in contrast, were neither significantly changed by BMP-9 overexpression nor by MCD-diet in these mice (Fig. 8A) and hepatic FGF19 mRNA levels did not correlate with NAS score in the patient samples (data not shown).

We further found that human hepatocytes cultured as monolayer show some induction of FGF21 by the combination of palmitic acid (PA) and oleic acid (OA) but not by linoleic acid (LA) or PA or OA alone (Fig. 8C). In monolayer cultured hepatocytes BMP-9 alone did not induce FGF21, however it enhanced the effect of PA but even reduced that of PA + OA. Hepatocytes cultured in the more physiological condition of organoids did not show any change in FGF21 expression, neither by fatty acids nor by BMP-9 or their combinations (Fig. 8D).

In summary these data do not support any direct induction of FGF21 expression by BMP-9 alone. Nevertheless, Fgf21 expression was decreased in the KO mice (Suppl. Fig. 3), implying that there might be some kind of indirect, systemic connection between BMP-9 levels and FGF21 expression, at least under already pathologic conditions like steatohepatitis.

Overall, our data suggest that counter-acting the BMP-9 decrease especially in the gut (e.g. by local application of BMP-9 mimetics) could exert beneficial, anti-diabetic effects by enhancing FGF19 expression.

#### 4. Discussion

Aim of the present study was to extend existing findings about a possible anti-diabetic function of BMP-9 in vivo and to investigate if this function might be related to modulations of the FGF-axis. Using different mouse strains there have been contradictory observations regarding general functions of BMP-9, e.g. during liver fibrogenesis as well as regarding the general BMP-9 KO phenotype (Breitkopf-Heinlein et al., 2017; Desroches-Castan et al., 2019) (see also below). So far it is not known which differences in the background strains are causing such opposite results but it is obvious that in order to translate any of these mouse-data to the human situation there is a great need for new results that are generated with patient samples. In the present study we therefore focused mainly on samples from a cohort of adipose patients and we were able to define two interesting new aspects of BMP-9's functions: 1. Besides the hepatic stellate cells in liver there exists a non-epithelial cell type in the small intestine (jejunum) that additionally expresses BMP-9 at high basal levels and this expression is dampened in diabetic patients. 2. In cells of the gut BMP-9 is directly upregulating the expression of the hepato-protective factor FGF19.

Recently published work investigated an additional, newly developed BMP-9 KO mouse (on a C57Bl/6 background) that was generated using CRISPR-Cas technology (Yang et al., 2020) and here an obese phenotype including steatosis was observed. For unknown reasons this was not the case in the BMP-9 KO mice that we investigated earlier (Breitkopf-Heinlein et al., 2017). Our mice are healthy and fertile and up to now no occurrence of any hepatic pathologies like steatosis were reported. For the present study we partially re-investigated the phenotype of these mice and could confirm normal levels of liver serum markers like ALT and AST at least at the age of 4–5 months (Suppl. Fig. 2). However, some other parameters (cholinesterase and alkaline phosphatase) as well as serum glucose were enhanced and the liver/body weight ratio was reduced.

Patients with metabolic syndrome or diabetes type 2 show decreased serum levels of BMP-9<sup>12, 13</sup>. This could indicate that the circulating BMP-9 protein was either exhausted due to enhanced demand under diabetic conditions or its expression was directly down-regulated, e.g. by enhanced levels of lipopolysaccharides (LPS; see below). In humans and mice, such decreased serum-levels were accompanied by reduced BMP-9 mRNA levels in the liver (Xu et al., 2017). We therefore aimed at addressing the question whether substitution of BMP-9 in order to compensate for a possible enhanced demand could be a new strategy to counter-act the development of diabetic conditions. Indeed, in the high fat diet (HFD) mouse model of NAFLD, over-expression of BMP-9 ameliorated the disease and improved glucose tolerance and IR (Yang et al., 2019). However, in a more inflammation-based model of NASH, the methionine-choline-deficiency (MCD) diet, BMP-9 aggravated the disease and enhanced the pro-inflammatory condition (Jiang et al., 2021; Li et al., 2019). The latter matching well with our previous observation that BMP-9 synergistically enhances the pro-inflammatory LPS-response in human macrophages (Gaitantzi et al., 2020). Therefore, BMP-9 supplementation might only be a promising approach during early phases of disease, before diabetes and/or steatohepatitis have already manifested.

We now confirmed down-regulation of BMP-9 serum levels in another animal model for diabetes, the streptozotocin (STZ)-induced rat model (Fig. 1). However, in contrast to the other models, we did not see any accompanying hepatic down-regulation of BMP-9 expression. The reason for this discrepancy might be that unlike the human situation, the STZ-mediated destruction of the insulin-producing beta-cells of the pancreas in our rats is an artificial situation leading to a much more rapid development (within 2–4 days) of diabetes (Akbarzadeh et al., 2007) than in humans. Possibly hepatic BMP-9 levels would drop at later time-points as well.

We performed Affymetrix microarray analyses of liver as well as small intestine and colon tissue samples from our BMP-9 KO mice and saw that besides the liver, there was also some BMP-9 expression detectable in the small intestine of the wild-type mice (Suppl. Fig. 3). However, since BMP-9 is only expressed in a small population of cells, in these whole-tissue samples both, hepatic as well as intestinal BMP-9 expression levels were rather low, possibly hitting the basal detection limit of the system. To isolate specifically the BMP-9 producing cells from liver and intestinal tissue and then compare directly the expression levels per cell will be an interesting task for future analyses. In the liver BMP-9 is known to be mainly produced by hepatic stellate cells (Breitkopf-Heinlein et al., 2017) and we previously showed that, BMP-9 is higher expressed in samples from human liver compared to gut tissue (Gaitantzi et al., 2020). ALK1, the main receptor for BMP-9, was in turn much higher expressed in gut than in liver. Likewise, ID1, one of the target genes of BMP-9 was also higher expressed in colon (Gaitantzi et al., 2020). These data support the concept that on the one side the gut might be an important target-organ for BMP-9 but, as our current data show, it also seems to be a source for BMP-9, in addition to the liver. To further support this assumption and to better translate the findings to the human situation, we collected blood, liver- and small intestine tissue samples from a cohort of adipose patients that obtained bariatric surgery in our department (n = 11 non-diabetic and 16 already diabetic patients; all with a BMI >40). We did not find any significant difference in serum levels of BMP-9 protein or hepatic BMP-9 mRNA between diabetic and non-diabetic patients of this cohort (Fig. 2A and B). This is somehow discrepant to the findings of Xu et al. who described decreased plasma levels of BMP-9 in patients with metabolic syndrome (Xu et al., 2017). The reason for this might be the fact that we did not compare completely healthy with diabetic patients but instead all our patients were obese and therefore they might as well already express less basal BMP-9 than healthy individuals. Most interestingly we were able to detect considerable expression of BMP-9 mRNA also in the small intestine samples of these patients and here the levels were strongly reduced in the diabetic patients (Fig. 2C), implying that intestinal BMP-9 might be

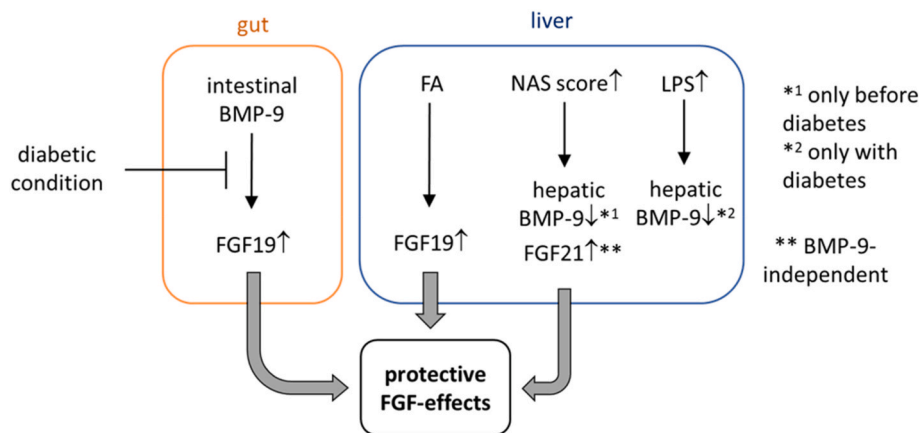


**Fig. 9. Scheme summarizing how BMP-9 acts in liver and gut to modulate protective FGF-actions in NAFLD conditions.** BMP-9 and FGF19 together form a gut-liver axis and thus influence metabolic homeostasis. BMP-9 is produced in both, the small intestine and the liver. In the small intestine BMP-9 locally induces expression of FGF19, especially if diabetes has not yet developed. The production of FGF19 in the liver in turn is enhanced by fatty acids, but not by BMP-9 directly. The expression of BMP-9 in the liver decreases in parallel to the inflammatory condition which in turn leads to more FGF21. The latter is most likely a BMP-9 independent effect. Rising LPS levels further down-regulate hepatic BMP-9, at least after diabetes has developed.

more relevant in this context than hepatic or circulating BMP-9. In situ hybridization analyses of tissue samples confirmed that there are some strongly BMP-9 expressing cells not only in the liver but also in the small intestine (Fig. 3). The exact identity of these cells remains to be defined, but they are clearly not located within the epithelial cell layer but between the epithelium and the muscular layers. By morphology (small and round) they might be some type of myeloid cell like dendritic cells or macrophages.

The hormone-like FGF19 subfamily, including FGF19 and FGF21, was described to positively act in multiple ways on glucose and fat metabolism (Babaknejad et al., 2018; Ryan et al., 2013; Dolegowska et al., 2019). Interestingly, FGF21 was reported to be induced in livers of obese mice upon injection of BMP-9<sup>11</sup>. In line with these data, we found reduced expression of FGF21 in liver-tissue of the BMP-9 KO mice whereas FGF15 (the murine analogue of FGF19) was strongly reduced especially in the small intestine of the KO mice (Suppl. Fig. 3B) fitting to previous data describing the small intestine as origin of FGF19 (Dolegowska et al., 2019; Zhang et al., 2015; Rinella et al., 2019). Bile acids secreted from liver were reported to stimulate the FGF19 production in the small intestine via Farnesoid-X-receptor activation, leading to its secretion into the blood (Song et al., 2009). FGF19 then binds to different FGF-receptors, in the liver especially to FGFR4 in combination with its co-receptor  $\beta$ -klotho (KLB) (Kurosu et al., 2007; Yang et al., 2012). As our array results demonstrate, FGF15 was strongly reduced in the small intestine of the KO mice, but not in the colon (Suppl. Fig. 3B), implying a differential expression of FGF15/19 in the different segments of the gut. It remains to be investigated if there is indeed higher FGF19 expression in the small intestine versus colon also in human samples.

Kim et al. postulated that BMP-9 led to enhanced hepatic FGF21 expression in mice in vivo (Kim et al., 2016). Our finding that FGF21 expression is reduced in BMP-9 KO mice would fit well with a role of BMP-9 as direct inducer of FGF21 expression. Kim et al. reported a direct induction of hepatic FGF21 by BMP-9 in vivo in obese mice that were fed an HFD. To analyse if this induction represents a general feature of BMP-9, already in otherwise healthy animals, we analyzed the livers of lean mice that were injected with a BMP-9 overexpressing adenovirus. In line with our in vitro findings using 2D and 3D hepatocyte cultures, we did not observe any significant BMP-9 dependent changes of FGF21 expression in the livers of these healthy mice (Fig. 8A) or in cultured hepatocytes (Fig. 8C and D). In contrast, only when inducing steatohepatitis in mice using the Methionine-Choline-deficient Diet (MCD), a model that involves an inflammatory reaction, hepatic FGF21 is indeed upregulated (Fig. 8A and published (Tanaka et al., 2015)), but also here, additional overexpression of BMP-9 did not further enhance FGF21 expression (Fig. 8A). Nevertheless, in the MCD model BMP-9 overexpression enhanced liver damage (Li et al., 2019) and this effect of BMP-9 depends on the presence of macrophages (Jiang et al., 2021). Therefore, one mechanism how BMP-9 controls hepatic FGF21 levels

could be mediated via crosstalk between inflammatory cells, like macrophages, and FGF21 producing cells. Such possible indirect regulation will be topic of future research.

In contrast to FGF21, BMP-9 clearly regulated FGF19 expression: whereas BMP-9 did not change its expression in hepatocytes (Fig. 4A and B), it strongly induced it in 3D-cultured gut epithelial cells (Fig. 4C). Fatty acids (FA) in contrast directly induced FGF19 expression specifically in hepatocytes (monolayer as well as organoids) but not in gut-organoids (Fig. 4). These data imply an intestine-specific enhancement of FGF19 possibly mainly by locally expressed (rather than systemic) BMP-9. In line with this conclusion the intestinal BMP-9 mRNA levels of our patients were significantly correlated with enhanced intestinal expression of FGF19 (Fig. 5). Interestingly, we did not find any correlation between intestinal or hepatic BMP-9 levels and FGF19 protein levels in the serum (Suppl. Fig. 4).

The reason for down-regulated expression of BMP-9 in the livers of diabetic patients might be that in these patients the serum levels of the gut-derived bacterial toxin lipopolysaccharide (LPS) are enhanced (Huang et al., 2019; Cani et al., 2008). As we previously showed, LPS directly down-regulates BMP-9 expression in hepatic stellate cells (Breitkopf-Heinlein et al., 2017). In line with this concept hepatic (but not intestinal) expression of BMP-9 was negatively correlated with serum LPS levels in our patient cohort, but this did not reach statistical significance and LPS serum levels were not significantly higher in the subgroup of already diabetic patients (Suppl. Fig. 4). Nevertheless, hepatic BMP-9 expression negatively correlated with the NAS score (Fig. 7) and this did reach significance levels but only in the subgroup of non-diabetic patients. In the diabetic patients this correlation was very weak, implying that possible anti-steatotic BMP-9 effects might be more relevant during the pre-diabetic stages. This assumption is also supported by our finding that intestinal BMP-9 expression correlates with that of the marker of intestinal barrier function, E-Cadherin, which was significantly reduced in our diabetic sub-cohort (Fig. 6).

In conclusion, our data support the concept of a beneficial function of BMP-9 under conditions of high-fat diet/obesity. As summarized in Fig. 9, our data imply that BMP-9 specifically expressed in the intestine upregulates local FGF19 expression but is at the same time itself down-regulated in the liver during steatosis development, which is possibly at least partially mediated by enhanced presence of LPS in the serum. Supplementation of BMP-9 or application of a BMP-9 mimetic might therefore represent a promising new therapy approach against steatosis and development of metabolic syndrome.

#### CRedit authorship contribution statement

**Stephan Drexler:** Data curation, Investigation, Validation, Visualization, Writing – review & editing. **Chen Cai:** Data curation, Investigation, Validation. **Anna-Lena Hartmann:** Investigation. **Denise**



**Moch:** Investigation. **Haristi Gaitantzi:** Methodology, Supervision. **Theresa Ney:** Investigation. **Malin Kraemer:** Investigation, Validation. **Yuan Chu:** Investigation. **Yuwei Zheng:** Investigation, Validation. **Mohammad Rahbari:** Writing – review & editing. **Annalena Treffs:** Formal analysis, Investigation. **Alena Reiser:** Investigation. **Bénédicte Lenoir:** Formal analysis. **Nektarios A. Valous:** Formal analysis. **Dirk Jäger:** Writing – review & editing. **Emrullah Birgin:** Resources, Writing – review & editing. **Tejas A. Sawant:** Investigation, Validation. **Qi Li:** Validation, Writing – review & editing. **Keshu Xu:** Resources. **Lingyue Dong:** Resources. **Mirko Otto:** Resources. **Timo Itzel:** Formal analysis. **Andreas Teufel:** Formal analysis, Investigation. **Norbert Gretz:** Writing – review & editing. **Lukas J.A.C. Hawinkels:** Investigation, Writing – review & editing. **Aránzazu Sánchez:** Resources, Writing – review & editing. **Blanca Herrera:** Resources, Writing – review & editing. **Rudolf Schubert:** Methodology, Resources, Writing – review & editing. **Han Moshage:** Writing – review & editing. **Christoph Reissfelder:** Funding acquisition. **Matthias P.A. Ebert:** Funding acquisition, Resources. **Nuh Rahbari:** Funding acquisition, Resources. **Katja Breitkopf-Heinlein:** Conceptualization, Funding acquisition, Project administration, Supervision, Visualization, Writing – original draft.

## Declaration of competing interest

The authors declare that they have no known competing financial interests or personal relationships that could have appeared to influence the work reported in this paper.

## Data availability

Data will be made available on request.

## Acknowledgements

The authors are thankful to Carolina De La Torre (Core Facility Platform Mannheim) for help with performing the microarray analyses and to Johannes Hoffmann and Christof Dormann (Department of Dermatology, Mannheim) for help with in situ hybridizations. K.B.-H. and H.G. were supported by funding from the Deutsche Forschungsgemeinschaft (DFG (German Research Foundation)-project No.: 393225014; 394046768-SFB1366). C.C. and Y. C. were fellows supported by the China Scholarship Council (CSC).

## Appendix A. Supplementary data

Supplementary data to this article can be found online at <https://doi.org/10.1016/j.mce.2023.111934>.

## References

- Akbarzadeh, A., Norouzi, D., Mehrabi, M.R., et al., 2007. Induction of diabetes by Streptozotocin in rats. *Indian J. Clin. Biochem.* 22 (2), 60–64.
- Angulo, P., 2002. Nonalcoholic fatty liver disease. *N. Engl. J. Med.* 346 (16), 1221–1231.
- Babaknejad, N., Nayeri, H., Hemmati, R., et al., 2018. An overview of FGF19 and FGF21: the therapeutic role in the treatment of the metabolic disorders and obesity. *Horm. Metab. Res.* 50 (6), 441–452.
- Bondow, B.J., Faber, M.L., Wojta, K.J., et al., 2012. E-cadherin is required for intestinal morphogenesis in the mouse. *Dev. Biol.* 371 (1), 1–12.
- Breitkopf-Heinlein, K., Meyer, C., König, C., et al., 2017. BMP-9 interferes with liver regeneration and promotes liver fibrosis. *Gut* 66 (5), 939–954.
- Cai, C., Itzel, T., Gaitantzi, H., et al., 2022. Identification of liver-derived bone morphogenetic protein (BMP)-9 as a potential new candidate for treatment of colorectal cancer. *J. Cell Mol. Med.* 26 (2), 343–353.
- Cani, P.D., Bibiloni, R., Knauf, C., et al., 2008. Changes in gut microbiota control metabolic endotoxemia-induced inflammation in high-fat diet-induced obesity and diabetes in mice. *Diabetes* 57 (6), 1470–1481.
- Carpino, G., Del Ben, M., Pastori, D., et al., 2020. Increased liver localization of lipopolysaccharides in human and experimental NAFLD. *Hepatology* 72 (2), 470–485.
- Carvalho, B.S., Irizarry, R.A., 2010. A framework for oligonucleotide microarray preprocessing. *Bioinformatics* 26 (19), 2363–2367.

- Chen, C., Grzegorzewski, K.J., Barash, S., et al., 2003. An integrated functional genomics screening program reveals a role for BMP-9 in glucose homeostasis. *Nat. Biotechnol.* 21 (3), 294–301.
- Degirolo, C., Sabba, C., Moschetta, A., 2016. Therapeutic potential of the endocrine fibroblast growth factors FGF19, FGF21 and FGF23. *Nat. Rev. Drug Discov.* 15 (1), 51–69.
- Desroches-Castan, A., Tillet, E., Ricard, N., et al., 2019. Differential consequences of Bmp9 deletion on sinusoidal endothelial cell differentiation and liver fibrosis in 129/ola and C57BL/6 mice. *Cells* 8 (9).
- Dolegowska, K., Marchelek-Mysliwiec, M., Nowosiad-Magda, M., et al., 2019. FGF19 subfamily members: FGF19 and FGF21. *J. Physiol. Biochem.* 75 (2), 229–240.
- Eslam, M., Newsome, P.N., Sarin, S.K., et al., 2020. A new definition for metabolic dysfunction-associated fatty liver disease: an international expert consensus statement. *J. Hepatol.* 73 (1), 202–209.
- Gaitantzi, H., Karch, J., Germann, L., et al., 2020. BMP-9 modulates the hepatic responses to LPS. *Cells* 9 (3).
- Godoy, P., Hengstler, J.G., Ilkavets, I., et al., 2009. Extracellular matrix modulates sensitivity of hepatocytes to fibroblastoid dedifferentiation and transforming growth factor beta-induced apoptosis. *Hepatology* 49 (6), 2031–2043.
- Goetz, R., Beenen, A., Ibrahim, O.A., et al., 2007. Molecular insights into the klotho-dependent, endocrine mode of action of fibroblast growth factor 19 subfamily members. *Mol. Cell Biol.* 27 (9), 3417–3428.
- Harrison, S.A., Rinella, M.E., Abdelmalek, M.F., et al., 2018. NGM282 for treatment of non-alcoholic steatohepatitis: a multicentre, randomised, double-blind, placebo-controlled, phase 2 trial. *Lancet* 391 (10126), 1174–1185.
- Herrera, B., Addante, A., Sanchez, A., 2017. BMP signalling at the crossroad of liver fibrosis and regeneration. *Int. J. Mol. Sci.* 19 (1).
- Huang, X., Yang, C., Luo, Y., et al., 2007. FGF4 prevents hyperlipidemia and insulin resistance but underlies high-fat diet induced fatty liver. *Diabetes* 56 (10), 2501–2510.
- Huang, X., Yan, D., Xu, M., et al., 2019. Interactive association of lipopolysaccharide and free fatty acid with the prevalence of type 2 diabetes: a community-based cross-sectional study. *J. Diabetes. Investig.* 10 (6), 1438–1446.
- Inagaki, T., Choi, M., Moschetta, A., et al., 2005. Fibroblast growth factor 15 functions as an enterohepatic signal to regulate bile acid homeostasis. *Cell Metabol.* 2 (4), 217–225.
- Jayashree, B., Bibin, Y.S., Prabhu, D., et al., 2014. Increased circulatory levels of lipopolysaccharide (LPS) and zonulin signify novel biomarkers of proinflammation in patients with type 2 diabetes. *Mol. Cell. Biochem.* 388 (1–2), 203–210.
- Jiang, Q., Li, Q., Liu, B., et al., 2021. BMP9 promotes methionine- and choline-deficient diet-induced nonalcoholic steatohepatitis in non-obese mice by enhancing NF- $\kappa$ B dependent macrophage polarization. *Int. Immunopharm.* 96, 107591.
- Kim, S., Choe, S., Lee, D.K., 2016. BMP-9 enhances fibroblast growth factor 21 expression and suppresses obesity. *Biochim. Biophys. Acta* 1862 (7), 1237–1246.
- Kuo, M.M., Kim, S., Tseng, C.Y., et al., 2014. BMP-9 as a potent brown adipogenic inducer with anti-obesity capacity. *Biomaterials* 35 (10), 3172–3179.
- Kurosu, H., Choi, M., Ogawa, Y., et al., 2007. Tissue-specific expression of betaKlotho and fibroblast growth factor (FGF) receptor isoforms determines metabolic activity of FGF19 and FGF21. *J. Biol. Chem.* 282 (37), 26687–26695.
- Li, Q., Liu, B., Breitkopf-Heinlein, K., et al., 2019. Adenovirus-mediated overexpression of bone morphogenetic protein9 promotes methionine choline deficiency-induced nonalcoholic steatohepatitis in nonobese mice. *Mol. Med. Rep.* 20 (3), 2743–2753.
- Miller, A.F., Harvey, S.A., Thies, R.S., et al., 2000. Bone morphogenetic protein-9. An autocrine/paracrine cytokine in the liver. *J. Biol. Chem.* 275 (24), 17937–17945.
- Moore, J.B., 2010. Non-alcoholic fatty liver disease: the hepatic consequence of obesity and the metabolic syndrome. *Proc. Nutr. Soc.* 69 (2), 211–220.
- Ogawa, Y., Kurosu, H., Yamamoto, M., et al., 2007. BetaKlotho is required for metabolic activity of fibroblast growth factor 21. *Proc. Natl. Acad. Sci. U. S. A.* 104 (18), 7432–7437.
- Paauwe, M., Heijkants, R.C., Oudt, C.H., et al., 2016. Endoglin targeting inhibits tumor angiogenesis and metastatic spread in breast cancer. *Oncogene* 35 (31), 4069–4079.
- Potthoff, M.J., Inagaki, T., Satapati, S., et al., 2009. FGF21 induces PGC-1 $\alpha$  and regulates carbohydrate and fatty acid metabolism during the adaptive starvation response. *Proc. Natl. Acad. Sci. U. S. A.* 106 (26), 10853–10858.
- Potthoff, M.J., Boney-Montoya, J., Choi, M., et al., 2011. FGF15/19 regulates hepatic glucose metabolism by inhibiting the CREB-PGC-1 $\alpha$  pathway. *Cell Metabol.* 13 (6), 729–738.
- Ricard, N., Ciaia, D., Levat, S., et al., 2012. BMP9 and BMP10 are critical for postnatal retinal vascular remodeling. *Blood* 119 (25), 6162–6171.
- Rinella, M.E., Trotter, J.F., Abdelmalek, M.F., et al., 2019. Rosuvastatin improves the FGF19 analogue NGM282-associated lipid changes in patients with non-alcoholic steatohepatitis. *J. Hepatol.* 70 (4), 735–744.
- Ritchie, M.E., Phipson, B., Wu, D., et al., 2015. Limma powers differential expression analyses for RNA-sequencing and microarray studies. *Nucleic Acids Res.* 43 (7), e47.
- Rowe, C., Gerrard, D.T., Jenkins, R., et al., 2013. Proteome-wide analyses of human hepatocytes during differentiation and dedifferentiation. *Hepatology* 58 (2), 799–809.
- Ryan, K.K., Kohli, R., Gutierrez-Aguilar, R., et al., 2013. Fibroblast growth factor-19 action in the brain reduces food intake and body weight and improves glucose tolerance in male rats. *Endocrinology* 154 (1), 9–15.
- Song, K.H., Li, T., Owsley, E., et al., 2009. Bile acids activate fibroblast growth factor 19 signaling in human hepatocytes to inhibit cholesterol 7 $\alpha$ -hydroxylase gene expression. *Hepatology* 49 (1), 297–305.
- Sun, Q.J., Cai, L.Y., Jian, J., et al., 2020. The role of bone morphogenetic protein 9 in nonalcoholic fatty liver disease in mice. *Front. Pharmacol.* 11, 605967.



- Tanaka, N., Takahashi, S., Zhang, Y., et al., 2015. Role of fibroblast growth factor 21 in the early stage of NASH induced by methionine- and choline-deficient diet. *Biochim. Biophys. Acta* 1852 (7), 1242–1252.
- Tang, N., Rao, S., Ying, Y., et al., 2020. New insights into BMP9 signaling in organ fibrosis. *Eur. J. Pharmacol.* 882, 173291.
- Townson, S.A., Martinez-Hackert, E., Greppi, C., et al., 2012. Specificity and structure of a high affinity activin receptor-like kinase 1 (ALK1) signaling complex. *J. Biol. Chem.* 287 (33), 27313–27325.
- Truksa, J., Peng, H., Lee, P., et al., 2006. Bone morphogenetic proteins 2, 4, and 9 stimulate murine hepcidin 1 expression independently of Hfe, transferrin receptor 2 (Tfr2), and IL-6. *Proc. Natl. Acad. Sci. U. S. A.* 103 (27), 10289–10293.
- van Baardewijk, L.J., van der Ende, J., Lissenberg-Thunnissen, S., et al., 2013. Circulating bone morphogenetic protein levels and delayed fracture healing. *Int. Orthop.* 37 (3), 523–527.
- Vizute, J., Camero, A., Malakouti, M., et al., 2017. Perspectives on nonalcoholic fatty liver disease: an overview of present and future therapies. *J Clin Transl Hepatol* 5 (1), 67–75.
- Xu, X., Li, X., Yang, G., et al., 2017. Circulating bone morphogenetic protein-9 in relation to metabolic syndrome and insulin resistance. *Sci. Rep.* 7 (1), 17529.
- Yang, C., Jin, C., Li, X., et al., 2012. Differential specificity of endocrine FGF19 and FGF21 to FGFR1 and FGFR4 in complex with KLB. *PLoS One* 7 (3), e33870.
- Yang, M., Liang, Z., Yang, M., et al., 2019. Role of bone morphogenetic protein-9 in the regulation of glucose and lipid metabolism. *Faseb. J.* 33 (9), 10077–10088.
- Yang, Z., Li, P., Shang, Q., et al., 2020. CRISPR-mediated BMP9 ablation promotes liver steatosis via the down-regulation of PPARalpha expression. *Sci. Adv.* 6 (48).
- Ye, X., Qi, J., Ren, G., et al., 2015. Long-lasting anti-diabetic efficacy of PEGylated FGF-21 and liraglutide in treatment of type 2 diabetic mice. *Endocrine* 49 (3), 683–692.
- Younossi, Z.M., Koenig, A.B., Abdelatif, D., et al., 2016. Global epidemiology of nonalcoholic fatty liver disease-Meta-analytic assessment of prevalence, incidence, and outcomes. *Hepatology* 64 (1), 73–84.
- Zhang, F., Yu, L., Lin, X., et al., 2015. Minireview: roles of fibroblast growth factors 19 and 21 in metabolic regulation and chronic diseases. *Mol. Endocrinol.* 29 (10), 1400–1413.